The mechanism of the cyclic switchover effect observed in electrochemical systems based on point contacts

V.A.Lykah[1], A.P.Pospelov[1], G.V.Kamarchuk[2], V.L.Vakula[2], E.S.Syrkin[2]

[1]National Technical University "Kharkiv Polytechnic Institute",
2 Kyrpychov Str., 61002 Kharkiv, Ukraine
[2]B.Verkin Institute for Low-Temperature Physics and Engineering,
National Academy of Sciences of Ukraine, 47 Nauky Ave.,
61103 Kharkiv, Ukraine

The paper proposes a mechanism of the cyclic switchover effect observed in electrochemical systems with point contacts used as nano-sized solid-state electrodes. The effect consists in cyclic processes of formation and dissolution of nano-dendrites synthesized in an electrolyte; it is generated by a new type of electrochemical electrode system — the gapless electrode system formed on the surface of the point-contact conduction channel. The main features of the cyclic switchover effect are analyzed in the framework of a self-oscillation model; the feedback effects are discussed. The paper also studies the properties of the gapless electrode system and examines the evolution of the conduction channel of the point-contact nanostructure. It is shown that the crucial condition for the unique evolution of the conduction channel is the formation of an electric arc responsible for the redistribution of the material and current in the electrochemical system. The proposed mechanism provides an adequate description of the experimentally observed phenomena and promises to be a useful tool for future studies. The results obtained in the paper can be used to develop a new generation of highly sensitive sensors based on the quantized conductance of dendritic point contacts immersed in electrolyte.

Keywords: Yanson point contact, nano-objects, gapless electrode system, cyclic switchover effect, self-oscillation, electrochemical arc.

Предложен механизм циклического электрохимического коммутационного эффекта, который наблюдается в электрохимических системах с точечными контактами. Эффект, заключающийся в чередовании процессов формирования и растворения нанодендритов, синтезируемых в электролите, возникает в новом типе электрохимической электродной системы — бесщелевой электродной системе, формирующейся на поверхности точечно-контактного канала проводимости. В рамках модели автоколебаний проанализированы основные особенности этого явления и обсуждены эффекты обратной связи. Исследованы свойства бесщелевой электродной системы и рассмотрена эволюция канала проводимости точечно-контактной наноструктуры. Показано, что критическим условием для реализации уникальной эволюции канала проводимости является образование электрической дуги, отвечающей за перераспределение вещества и тока в электрохимической системе. Предложенный механизм адекватно описывает экспериментально наблюдаемые явления и несомненно будет полезен для последующих исследований. Полученные в работе результаты могут быть использованы для разработки нового поколения высокочувствительных сенсоров, построенных на использовании квантования проводимости дендритных точечных контактов, погруженных в электролит.

Механізм циклічного електрохімічного комутаційного ефекту, що спостерігається в електрохімічних системах на основі точкових контактів. *В.О.Ликах, О.П.Поспєлов, Г.В.Камарчук, В.Л.Вакула, Є.С.Сиркін.*

Запропонований механізм циклічного електрохімічного комутаційного ефекту, що спостерігається в електрохімічних системах з точковими контактами, використаними в якості нанорозмірних твердотільних електродів. Ефект, що полягає у чергуванні процесів формування та розчинення нанодендритів, які синтезуються в електроліті, виникає у новому типі електрохімічної електродної системи і безщілинній електродній системі, що формується на поверхні точково-контактного каналу провідності. У рамках моделі автоколивань проаналізовано основні особливості цього явища та обговорено ефекти зворотного зв'язку. Досліджено властивості безщілинної електродної системи та розглянуто еволюцію каналу провідності точково-контактної наноструктури. Показано, що критичною умовою для реалізації унікальної еволюції каналу провідності є утворення електричної дуги, що відповідає за перерозподіл речовини та струму в електрохімічній системі. Запропонований механізм адекватно описує експериментально спостережувані явища та безперечно буде корисним для подальших досліджень. Отримані результати можуть бути використані для розробки нового покоління високочутливих сенсорів, побудованих на використанні квантування провідності дендритних точкових контактів, занурених в електроліт.

1. Introduction

One of the most active areas of modern fundamental and applied researches is development of advanced nanotechnologies. Yanson point contacts [1] are among the promising objects employed to achieve the goal [2–4]. Unlike many theoretical models proposed by a number of authors [5–8], the Yanson point contacts are a real technical product manufactured using the knowledge acquired and accumulated in the process of development of the Yanson point-contact spectroscopy. Being characterized by unique quantum properties, these nano-objects, however, can be relatively easily produced using some simple technological know-hows of the Yanson point-contact spectroscopy [3, 9]. A distinctive feature of the Yanson point contacts is their strict compliance with some clearly formulated quality criteria [9]. These criteria are needed to produce samples with predetermined or predictable properties. As a result, the nature of the Yanson point contacts is drastically different from that of conventional electric contacts. The original physical properties and applications of the Yanson point contacts include, among others, their spectroscopic capabilities [9, 10], quantized conductance [11–13], and a gas-sensitive effect [14, 15]. The unique nature of the Yanson point contacts not only creates the necessary conditions for them to be used as an efficient tool to study various electric and quantum effects [4], but also lays the foundation for the development of new low-cost advanced technologies. The practical use of the Yanson point contacts can be illustrated by the development of sensors with unique parameters [3] and the creation of an innovative technology of real-time detection of carcinogenic strains of *Helicobacter pylori*, which has already been successfully tested [16].

Immersion of the point contacts into a conducting liquid medium opens up new opportunities never known before. Dendritic point contacts produced this way display new fundamental properties which may lead to a breakthrough in nanotechnologies [17, 18]. They have been developed with the purpose of creating objects with a room-temperature electron mean free path greater than the contact diameter. The dendritic point contacts possess quantum properties and exhibit electronic and atomic shell effects at room temperature. They are characterized by ballistic electronic conductivity. These fundamental features imply a priori that the dendritic point contacts also have spectral properties [19]; that's why they belong to the family of the Yanson point contacts, which, together with other contact structures, are used in the Yanson point-contact spectroscopy.

In this paper, we discuss a new effect obtained with the dendritic point contacts — the *cyclic switchover effect* in electrochemical systems based on the Yanson point contacts [18]. As it is shown in [17, 18, 20, 21], the effect is generated by a new type of the electrochemical electrode system — the *gapless electrode system* (GES), previously known as *elongated electrochemical element* [17, 18, 22], which is formed on the surface of the conductivity channel of a point contact immersed into a liquid medium. The importance of studying the GES and the cyclic processes related to it is largely due

to the lack of comprehensive information on the cyclic processes in electrochemistry. Discovery of a new cyclic process is of great interest to specialists in different fields. The cyclic effect of electrochemical point-contact commutation opens new facets to the understanding of physics and chemistry of nanostructured electrode systems and broadens the prospects of their practical use.

When dealing with synthesis of the dendritic point contacts and with the cyclic switchover effect, one has to consider the processes which occur at the macro- and nano-levels. The cyclic switchover effect is a series of alternating processes induced by electric field: growth and dissolution of a dendritic point contact in electrolyte [18]. The macro-level processes include the initial dendrite growth. Once the dendrite tip reaches the counterelectrode (anvil), a nanostructure emerges — the dendritic Yanson point contact [3] — and the subsequent processes of the cyclic switchover effect are those typical of quantum conducting systems [23]. This combination of the processes occurring at both macro- and nano-levels is very unusual and needs an integrated approach.

Here we propose a mechanism of the observed cyclic switchover effect. We demonstrate the self-oscillation nature of the effect, reveal and analyze its main characteristics. The proposed mechanism describes adequately the experimental situation [17, 18] and promises to be useful for explanation of new effects obtained with dendritic Yanson point contacts. It should be noted that the processes of formation and dissolution of the conductivity channel of the dendritic Yanson point contact have the character of a self-oscillation and do not require any differently directed external forces [18]. To start the processes, it is enough to apply an electric field to the system. This is one of the main differences from the processes in which the contacts are produced using the traditional electrochemical technology of deposition or dissolution of a metal [24, 25]. In the case of the classic electrochemical technology, the transition from metal deposition to its dissolution is attained by manually reversing polarity of the main and auxiliary electrodes, while the cyclic switchover effect is only a result of the permanent action of an electric field [17, 18].
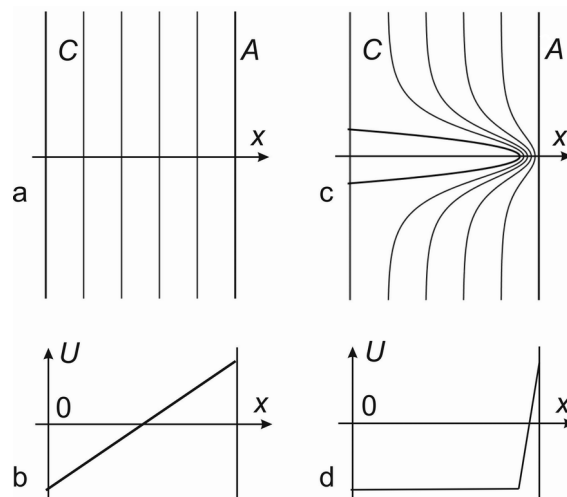

Fig. 1. Model of the system. Geometry of the experiment. Parallel planes are electrodes: cathode (C), anode (A). Upper-left section (a) — uniform conducting solution, parallel lines between cathode and anode are equipotential surfaces. Lower-left section (b) — uniform potential drop in the solution. Upper-right section (c) — part of the conductivity channel during its growth or after its break. Cathode and the part of the conductivity channel constitute a single continuous metallic equipotential surface. Curved lines — cross-sections of equipotential surfaces in electrolyte, distorted if compared to those in Fig. 1a. Lower-right section (d) — nonuniform potential drop along the axis of the remaining part of the conductivity channel and electrolyte.

2. Model

Consider a system which is equivalent to a plane capacitor filled with an electrolyte. The equipotential surfaces between the capacitor planes are equidistant and parallel to the planes. The linear voltage vs. distance dependence is shown in Fig. 1a,b. The specificity of the system is that the planes are connected through a cylindrical conductor which is normal to them. The conductor can be used to model the conductivity channel of the Yanson point contact [4, 9].

Formation of a GES is a characteristic result of the influence of this linear potential distribution on surface electrochemical phenomena [18, 21, 22]. Note, that the GES includes two sections on the conductor surface which are its integral structural parts: the cathode section, concerned with the processes of deposition and reduction, and the anode one, where the processes of dissolution and oxidation take place. These two sections are separated by a polarity inversion boundary — a line on the surface with

no directed electrode processes. Let us take the so-called zero point, which coincides with the inversion boundary, as the reference point for the potential. The potential U at a given point is the potential drop between the point and the inversion boundary. The rate at which ions pass through the metal-solution interface does not depend on the interface orientation, being only dependent on the potential at the given point on the interface with respect to the inversion boundary. This independence on the interface orientation is absolutely natural, since the potential at a point is a scalar value. It can be seen from Fig. 1a, b that in the case of a linear dependence, the zero point of the uniform channel is initially equidistant from both of the channel banks. In the process of dissolution, the zero point moves (see Fig. 1c, d).

For small deviations of the potential from the zero point, the expression for the maximum current density can be given as follows [26]:

$$j = j_0 zFU/2RT. \qquad (1)$$

Here j_0 is the exchange current density, z is the number of electrons transferred simultaneously through the metal — solution interface, F is the Faraday constant, U is the potential drop between the banks, R is the universal gas constant, and T is the temperature. As U grows, the current vs. potential dependence becomes nonlinear.

The voltage changes along the whole channel, which means the conditions for deposition (dissolution) change too. The initial distributions of the channel mass and cross-section which are uniform throughout the channel became no longer uniform when the channel carries a current. As a result, the conductivity channel can partly dissolve. Having no contact with the anode, the surface of the cylindrical conductor is virtually equipotential (see Fig. 1c), since the resistance of the electrolyte and the metal — electrolyte interface exceeds greatly that of the metallic channel [18]. The conducting channel has a potential equal (or close) to that of the anode, giving thus rise to processes of channel growth which continue until the contact with the anode is there again. The contact with the anode and the flowing current change the situation drastically — the GES comes into the play. This new cycle starts with the polarization inversion boundary at the geometrical centre of the conductivity channel

of the newly formed Yanson point contact. There is again the initial uniform potential drop along the channel; the areas of ion dissolution and deposition reappear.

The relation between the density of ion current j and the carrier concentration n, carrier charge q, and velocity v of ion ordered motion in the electric field is:

$$j = q_1 n_1 v_1 + q_2 n_2 v_2. \qquad (2)$$

Here the subscripts 1 and 2 refer to positive and negative ions in the solution. In our system, the dissolution — transfer — deposition processes are related to the ion subsystem of the metal. Therefore, the current depends on the number of ions transferred from the metal surface to the solution in unit time. It can be seen from Eqs. (1) and (2) that the ion number is proportional to the potential at a given point of the channel (as we have already said, by the potential we mean a potential drop between a given point and a point on the inversion boundary).

In accordance with Eqs. (1) and (2), the maximum dissolution rate is observed in the area of contact with the positive bank. Equation (1) describes the current density for dissolution (deposition) of metal ions between the electrode and electrolyte as a function of the potential. Equation (2) yields the current density inside the electrolyte. It can be seen that the dissolution rate grows as the potential increases, i.e. as the distance from the anode decreases. Therefore, the current density in the electrolyte (2) also grows due to the current continuity. Near the negative bank of the channel, the dissolution rate reaches its maximum value. A change in the channel shape results in a nonuniform distribution of resistance and, therefore, in a nonuniform dependence of the potential drop. Narrowing of the channel shifts the zero point towards the anode. This means, as the process develops, the main portion of the potential drop between the banks shifts in the same direction. The intensity of the processes considered above grows significantly. Equipotential surfaces in the liquid near the contact surface adjust themselves to the equipotential surfaces in the contact. A denser arrangement of the equipotential surfaces corresponds to a higher intensity of the electric field; the velocity of ion motion is quickly increased in a small area adjacent to the positive bank, since the electric field grows there. The process of heat removal from the point contacts was analyzed in detail in [27] (see also [28] on heat trans-

mission between two media). At such great electric fields, direct conductivity in the electrode and in the solution is interrupted due to electrochemical processes of dissolution rather than heat phenomena. In the direct-current mode realized in our experiment, the potential drop and overheating reach their critical values when the contact gets lost. The system starts operating in the oscillation regime with alternating processes of growth and dissolution.

The greater the current maintained in the system (in dc mode), the longer is the section of the channel which may dissolve. If, after the contact is lost, there is still a part of the channel left near the anode, it is first to dissolve because of the high concentration of electric field between the cathode and the anode near the sharp tip of the electrode. During the dissolution of the conductivity channel, all of the current between the cathode and the anode contributes to depositing the metal on the cathode to quickly restore the contact. In the experiment [18], the break of the channel is accompanied by a huge increase in the resistance observed for a short period of time (less than 0.1 s) followed by a quick recovery of the broken part. The dissolution of the channel occurs over quite a long period of time (1 to 10 s). The long duration of this phase is due to the fact that during the dissolution of the channel near the anode, the electrolysis current remains pretty small (much smaller than the current flowing directly through the channel).

3. Formation of arc discharge

The break of the conductivity channel results in a sharp increase in the resistance of the medium followed by an arc discharge. The arc emerges when the gap in the conductivity channel is as small as one or few monomolecular layers of the solution. A large part of electrons can get through the gap without dissipating their energy. At the initial stage of the arc discharge, during the arc formation, electron energy is mostly transformed into heat in the metallic electrode. The energy of one electron, eU, is not enough to knock out a metal atom. It spreads over a certain layer of the crystal near its surface. If the flux of energy brought by electrons is much greater than the flux of heat removed from the system, an overheated area emerges near the anode. Heat removal in the point contacts can be hindered due to their geometry and the cut-off effect [29]; that is a cut-off of the high-

frequency part of the phonon spectrum (the spectrum of acoustic lattice vibrations lies within the range from zero to the Debye frequency). So, at temperatures exceeding the Debye temperature, the removal of heat into the inner part of the electrode becomes much less efficient. Almost all energy brought by electrons remains in the relatively thin layer near the electrode surface. The average temperature of this heated near-surface layer can be estimated by comparing the energy eU delivered by one electron with the mean energy of heat motion of a crystal atom, which is close to kT by the order of magnitude:

$$T = eUN_e / kN_{at}. \qquad (3)$$

Here N_{at} is the number of atoms in the overheated near-surface area of the electrode; N_e is the number of electrons which reached the electrode surface. For estimation, we take these experimental data [18]: $I = 20 \ \mu A = 2 \cdot 10^{-5}$ A, $R_R = 12.9$ kΩ (resistance of a single-atom contact equivalent to one conductance quantum), $U = IR_R = 0.26$ V. The initial (minimum) estimation can be calculated under the assumption that the number of atoms in the overheated layer is equal to that of the electrons brought to the electrode, $N_e = N_{at}$. This is indeed the minimum possible value, because for our current values, the condition $N_e > N_{at}$ (and even $N_e >> N_{at}$) is fulfilled rather quickly. Hence, we arrive to the temperature T of about 3200 K. The huge electron flux I/e (which is of the order of magnitude of 10^{13} s^{-1}) leads to a fast and intense heating of the anode surface up to the boiling point of the anode material. The electron flux of 10^{13} s^{-1} falls on a tiny surface. After the dissolution (break) of the conductivity channel, the area of the tip of the broken channel is 1 to 100 nm^2. With the initial gap of ~ 1 nm, the current density is $j = I/S$ ~ (1÷100)·10^{12} A/m^2. The electron flux per unit area can be estimated to be j/e ~ (1÷100)·10^{31} m^{-2}. This means that the electron flux reduced to the size of the point contact is characterized by a huge concentration of the produced energy, because, according to the Joule-Lenz law, the specific heat is $w = rj^2$, where r is the resistivity of the medium.

With the electric arc already formed, i.e. with high electron fluxes and large overheating of the surface, the energy removed

from the system and lost to heating the metal is not significant any more — all energy of the electron beam, jU (per unit area), is consumed to evaporate the anode. The rate at which the metal vapour flows away from the surface can be estimated with the following expression [30]:

$$u_{Me} = jU / Lr_{Me}. \qquad (4)$$

Here L is the specific heat of evaporation and r_{Me} is the solid metal density. The vapour density r_{Me+} can be converted into the concentration of ions: $n_{Me} = (n_{Me+} - n_{Me-})$, where $n_{Me} = r_{Me}/m_{at}$ and n_{Me} is the concentration of the vapour gone into the gas-plasma bubble from the electrode. Then the metal vapour pressure in the bubble can be presented as $P_{Me} = n_{Me}kT$. We should also take into account the evaporation of the cathode due to knocking particles out of its surface when the arc is on.

In the *dc* mode, the apparatus maintains the same current strength. In the experiments [18], when the conductivity channel gets broken (dissolved), its maximum resistance (R_R) is observed to be about $R_R = 40$ MΩ [18] with the potential amounting to $U = IR_R = 8 \cdot 10^3$ V. Then the energy transferred to the electrode atoms corresponds to the temperature of heat motion which is several orders of magnitude higher than the value obtained above. Of course, such a high temperature is not reached since the critical overheating and ignition of the arc take place at much lower values. The high resistance (about 40 MΩ) can be assigned to both the low conductivity of the electrolyte solution within a quite wide gap in the conducting metallic channel and the formation of a solution-electrode interface after a large portion of the channel breaks. In this case, the heat generation is distributed over the volume of the electrolyte contained between the needle and the anode.

At the point when the narrowest part of the conductivity channel gets broken due to dissolution, the potential drop rapidly redistributes itself in such a way that much of it is now concentrated near the break. The maximum value of resistance is not reached at once. At the same time, the maximum potential drop exists within the gap in the metallic contact where optimal conditions for the start of heating and evaporation of atoms are created at the broken ends of the conducting metallic contact (ignition of the electric arc) [31]. As the gap grows during

the arc discharge, the resistance of the electric circuit increases, so do the voltage and heat generation; the estimated minimum temperature for an atom to be pulled out of the contact was 3200 K. This is, in fact, the description of the process of ignition of an electric arc in the gap of a metallic channel immersed in an electrolyte. At temperatures of the order of magnitude of 10^3 K, the liquid evaporates and the current transforms the vapoury mixture of atoms of the metal and molecules of the liquid into a plasma (for example, the boiling point of copper, which is widely used to produce point contacts, is close to 2900 K [32]). The arc discharge composed of a gas-vapour shell, and the spectral lines of metal ions and dissociated components of the electrolyte were observed experimentally [31]. A stationary mode of the arc discharge is achieved under the following condition:

$$P_{bubble} = P_{ext}, \qquad (5)$$

i.e. under the condition of equilibrium of the surface of the gas-plasma bubble, where

$$P_{ext} = P_{atm} + P_{Gs} + P_{cap},$$

$$P_{bubble} = P_{Cu} + P_{H} + P_{O} + P_{H_2O} + \dots.$$

Here, the overall pressure P_{bubble} inside the bubble of vapour, and ions of the metal P_{Cu}, and water P_{H_2O}, and dissociation products P_{H} and P_{O} counterbalances the external pressure P_{ext} which includes atmospheric P_{atm}, hydrostatic P_{Gs}, and capillary P_{cap} components. This condition is similar to the requirement for boiling [33], where P is the saturation vapour pressure.

In the process of arc discharge, the length of the electric arc grows, so does the lateral surface of the bubble, i.e. there is an increase in the number of metal ions entering into the solution from the plasma. Therefore, the metal vapour pressure $P_{Me} = n_{Me}kT$ decreases due to the decrease in the concentration n of metal atoms in the arc bubble. When the following condition is met: $P_{bubble} < P_{ext}$, the bubble containing the arc collapses and the discharge stops. Electric arc or electrical discharge in solutions, known as *electrochemical arc* or *electrochemical arc discharge*, is used in various technical applications [34, 35].

At the next stage, an elongated area with a high concentration of metal ions is formed in the place of the arc after the bubble col-
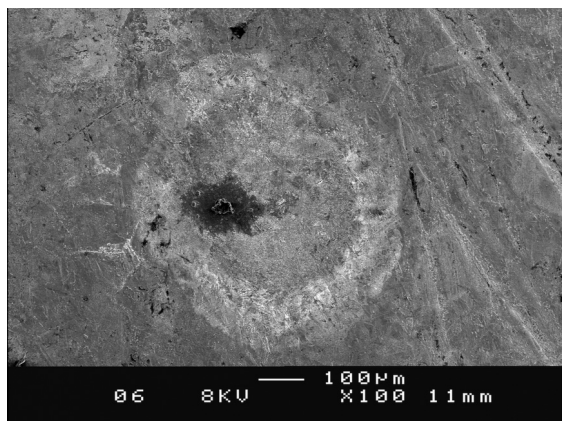
Fig. 2. SEM image of a crater on the anode surface (central dark area). The light circle around is the dry residue of electrolyte.
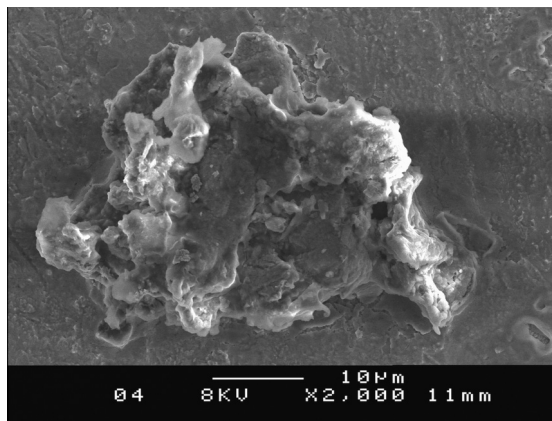

Fig. 3. SEM image of the salt-coated remnant of the conducting channel of a dendritic Yanson point contact in the central part of the crater (see Fig. 2).

lapses; it contains ions which penetrated into the electrolyte after hitting the cavity surface during the arc discharge and those residing in that area at the time of collapse. Almost all of the needle metal evaporated during the arc discharge ends up in the solution. It can also contain some hydrogen and oxygen ions left from the plasma as well as combustion products. The concentration n of charge carriers produced this way inside the area can be several orders of magnitude higher than the concentration of charge carriers in the solution beyond it; this was observed experimentally [31]. So, in accordance with Eq. (2), a filament characterized by a high density of current lines is formed in the place of the arc.

One end of the filament is at the needle tip (conductivity channel cathode) and it grows fast due to the high current density here. The other end of the high-conductivity filament is in contact with the anode surface and, due to the current continuity, should cause a fast dissolution of the narrow part of the flat anode; as a result, an experimentally observable crater is formed (see Fig. 2). If the dissolution at the anode maintains a sufficiently high concentration of ions in the filament, the needle tip can grow as far as to reach the anode and restore the lost contact over a pretty large channel cross-section area in a short period of time. In the experiment described in [18], currents from 1 to 50 μA were used. On the average, the channel cross section and conductance were observed to increase with increasing current. In the proposed model, this means that as the current grows, the power of the arc increases; then, after the arc goes out, it is the concentration of carriers in the filament that keeps growing.

4. Synthesis of dendrites

We would like to emphasize here that we are able to clearly discriminate between two opposite processes. One of them is the arc discharge in the solution. The other is a purely electrochemical process of fast deposition (restoration) of the conducting channel from the high-concentration solution of the metal in the electrolyte. The latter process can be called *fast electrochemical deposition or filamentary electrochemical deposition*, since it occurs within the filament with a high concentration of metal ions.

Figures 2 and 3 show the state of the anode (anvil) after observation of the cyclic switchover effect in [18]. To have a more comprehensive insight into the transformations which occur at the electrodes of a dendritic point contact, one should examine Figs. 2 and 3 together with Fig. 2 in [18], which shows a SEM image of a needle-shaped electrode (cathode) and dendrites forming a Yanson point contact. Dimensions and shapes of the object can clearly be seen from Figs. 2 and 3.

As the crater deepens, the conducting channel inside it gets partly screened; this results in a lower density of the dissolution current. This leads to a break of the direct-conductivity channel above the contact of the dendrite tip with the anode surface inside the crater (see Fig. 3). The temporal change in the channel resistance has a cyclic self-oscillation character [18].

Our concept allows to distinguishing the following characteristic phases of one self-oscillation cycle:

1. When the conducting channel of a dendritic Yanson point contact has already

been formed, a part of it starts dissolving due to electrolysis (GES regime). This is the longest process of the cycle lasting from 1 to 10 sec.

2. Direct conductivity of the point contact gets broken.

3. Electric plasma arc goes on (switchover process).

4. Fast process of arc discharge.

5. Collapse, or extinction, of the arc (another switchover).

6. Electrochemical-filament process, that is a fast galvanic growth of the conducting metallic channel (cathode) accompanied by dissolution of the anode. The filament in the plasma is formed as a result of the filament instability [36−38]. In our system, the filament is "inherited" from the electric arc.

7. The conducting channel contacts the anode (switchover followed by formation of a GES structure).

Processes 2 to 7 occur so fast that they have not been registered yet (with measurements performed at a registration rate of 10 points per second [18]). The total duration of the processes 2 to 7 can be estimated to be less than 0.1 s.

The choice of the parameter which could be used to describe the self-oscillation of the system is not trivial. Let us compare the system under consideration with the self-oscillation of a clock pendulum. A self-oscillating system must include three components [39, 40]:

1. An oscillating body.
2. A source of energy (energy supply).
3. A feedback mechanism.

In a clock, the energy supply is provided by the potential energy of the weight suspended on a chain, the oscillating body is the pendulum, and the feedback mechanism is the anchor escapement. A positive feedback triggers the energy supply in the right phase of the oscillation, thus increasing the oscillation amplitude or maintaining the limit cycle.

5. Phase portraits

The phase portrait of a clock is well known [39], it is drawn in coordinates x and v (see Fig. 4). Without a supply of external energy, the pendulum oscillation damping follows an elliptic spiral. The jump at the feedback point in Fig. 4 shows energy supply at the middle point of the trajectory (a jump in velocity).

By analogy with the x and v coordinates, let us take coordinates m and dm/dt, m
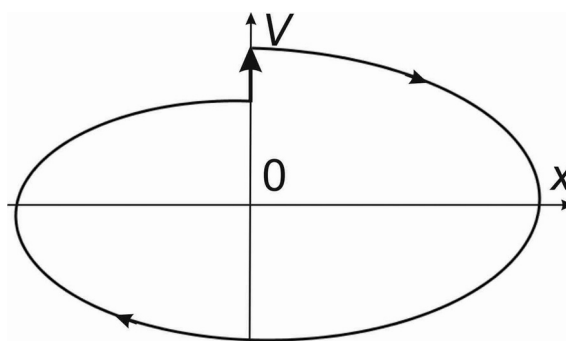

Fig. 4. Phase portrait (limit cycle) of oscillation of a clock pendulum.

being the variable portion of the mass of the conducting metallic channel. The main portion of the mass does not change at all or changes very slowly. Therefore, we only take the portion of the channel mass that vanishes completely and then reappears during a stationary self-oscillation. This implies a shift of the origin of coordinates along the mass axis. Fig. 5 shows the proposed phase portrait of the analyzed system. It is in fact a generalization of a simpler system shown in Fig. 4. In the self-oscillation process considered here, the fluxes of external energy and mass are originated by the electrolysis current along the surface of the conducting channel. The oscillating body is a portion of the mass of the conducting metallic channel. The feedback apparently includes three switchover processes — 3, 5, and 7 in the phase portrait in Fig. 5.

The mass reduction during the oscillation occurs in the processes 1 and 4 of the slow dissolution and fast arc-discharge-induced evaporation. The mass growth takes place in the oscillation during the electrolytic growth (process 6 on the phase portrait). Processes 1, 4, and 6, as has already been mentioned above, are characterized by different rates, the difference being as high as several orders of magnitude. Evident feedback mechanisms correspond to processes 5 and 7. The process 5 (collapse of the electric arc discharge) describes the switchover from evaporation of the channel to its growth. The process 7 (contact of the conducting channel with the anode) is after the switchover from a fast electrolytic growth of the channel to its slow electrolytic dissolution. The switchover process 3 (start of the electric arc discharge) corresponds to the onset of a fast inertial phase of evaporation of the conducting metallic channel. It is this process of the arc discharge that is responsible for the large amplitude of the self-oscillation. Were it not for this process,
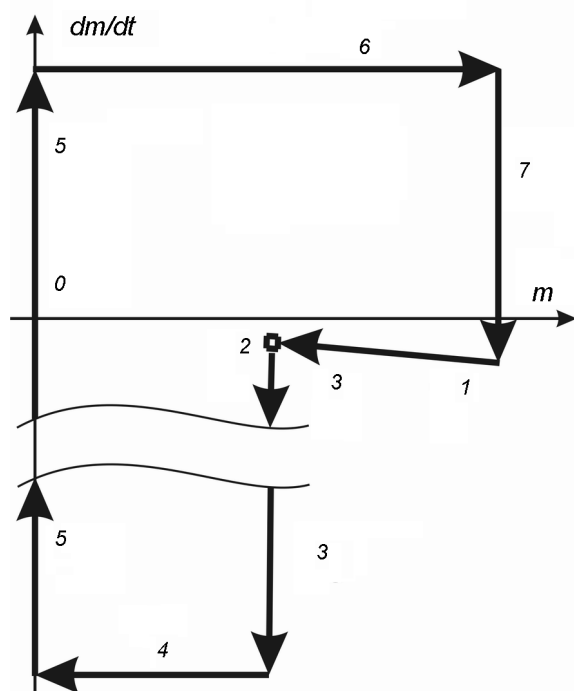
Fig. 5. Phase portrait of self-oscillation of the variable portion of the mass of the conducting metallic channel of a Yanson point contact immersed in electrolyte. *1* — slow dissolution caused by electrolysis; *2* — break of direct conductivity of the point contact; *3* — start of arc discharge (switchover process, feedback); *4* — sharp process of arc discharge; *5* — collapse, or extinction, of the arc (discharge process, feedback); *6* — electrochemical-filament process, i.e. a sharp galvanic growth; *7* — contact of the conducting channel with the anode (switchover process, feedback).

the self-oscillation would probably have smaller amplitude. With growing current, the oscillation amplitude in the phase portrait in Fig. 4 can increase by a few orders of magnitude. A large portion of the oscillating channel mass probably evaporates during the arc discharge, and the slow galvanic dissolution only creates the conditions necessary for the discharge to start. In stationary self-oscillations, the mass difference between the processes 1 to 4 and 6 is made up for with the anode material.

The proposed new approach allows one to reveal the main phases of the microscopic mechanism of the cyclic self-oscillation process realized in the system of *dendritic Yanson point contact — electrolyte.*

6. Conclusions

A mechanism of the cyclic switchover effect observed in electrochemical systems based on Yanson point contacts is proposed. The new approach is a result of the study of the gapless electrode system formed in an electric field on the surface of the conductivity channel of a dendritic Yanson point contact immersed in electrolyte. The evolution process of a uniform conductivity channel of the analyzed nanostructure is considered. In the galvanostatic regime, the dissolution takes place at the rates which increase towards the anode. The dissolution enhancement is accompanied by an increase in the contact resistance with the channel cross-section decreasing down to the size of an atom. When the channel breaks, the highest concentration of the electric field is achieved at the tip of the needle making it thus possible for a plasma electric arc to emerge. The idea of arc formation as a phase in the evolution of a dendritic Yanson point contact immersed in a solution is proposed for the first time. Also, for the first time, feedback processes are taken to describe the main phases of the cyclic self-oscillation effect. The proposed mechanism provides an adequate description of the experimentally observed phenomena and promises to be a useful tool for future research of conductance quantization of dendritic point contacts and development of new types of quantum sensors [41].

References

1. I.K.Yanson, *J.Exp.Theor.Phys.*, **39**, 506 (1974).
2. I.K.Yanson, Yu.G.Naidyuk, V.V.Fisun et al., *Nano Lett.*, **7**, 927 (2007).
3. G.V.Kamarchuk, A.P.Pospelov, L.V.Kamarchuk, I.G.Kushch, in: V.A.Karachevtsev (ed.), Nanobiophysics: Fundamentals and Applications, Pan Stanford Publishing, Singapore (2015), p.327.
4. Yu.G.Naidyuk, I.K.Yanson, Point-contact Spectroscopy, Springer, New York (1965).
5. Yu.V.Sharvin, *J.Exp.Theor.Phys.*, **21**, 655 (1965).
6. I.O.Kulik, A.N.Omel'yanchuk, R.I.Shekhter, *Sov.J.Low Temp.Phys.*, **3**, 740 (1977).
7. I.O.Kulik, I.K.Yanson, *Sov.J.Low Temp. Phys.*, **4**, 596 (1978).
8. I.O.Kulik, R.I.Shekhter, A.G.Shkorbatov, *J. Exp.Theor.Phys.*, **54**, 1130 (1981).

9. A.V.Khotkevich, I.K.Yanson, Atlas of Point Contact Spectra of Electron-phonon Interactions in Metals, Kluwer Academic Publishers, Boston, Dordrecht, London (1995).

10. G.V.Kamarchuk, A.V.Khotkevich, V.M.Bagatsky et al., *Phys. Rev. B*, **63**, 073107 (2001).

11. L.I.Glazman, G.B.Lesovik, D.E.Khmel'nitskii, R.I.Shekhter, *JETP Lett.*, **48**, 238 (1988).

12. E.N.Bogachek, A.M.Zagoskin, I.O.Kulik, *Sov. J. Low Temp. Phys.*, **16**, 796 (1990).

13. J.M.Krans, J.M.van Ruitenbeek, V.V.Fisun et al., *Nature (London, UK)*, **375**, 767 (1995).

14. G.V.Kamarchuk, O.P.Pospelov, A.V.Yeremenko et al., *Europhys. Lett.*, **76**, 575 (2006).

15. G.V.Kamarchuk, I.G.Kolobov, A.V.Khotkevich et al., *Sens. Actuators B*, **134**, 1022 (2008).

16. I.Kushch, N.Korenev, L.Kamarchuk et al., *J. Breath Res.*, **9**, 047109 (2015).

17. G.V.Kamarchuk, A.P.Pospelov, A.V.Savitsky, L.V.Koval, *Low Temp. Phys.*, **40**, 937 (2014).

18. A.P.Pospelov, A.I.Pilipenko, G.V.Kamarchuk et al., *J. Phys. Chem. C*, **119**, 632 (2015).

19. A.I.Yanson, Dissertation, Leiden University (2001).

20. A.I.Pilipenko, A.P.Pospelov, G.V.Kamarchuk et al., *Functional Materials*, **18**, 324 (2011).

21. A.P.Pospelov, G.V.Kamarchuk, A.V.Savytskyi et al., *Functional Materials*, **24**, 463 (2017).

22. A.P.Pospelov, G.V.Kamarchuk, Yu.L.Alexandrov et al., in: E.C.Faulques, D.L.Perry, A.V.Yeremenko (eds.), Spectroscopy of Emerging materials. Kluwer Academic Publishers, Boston, Dordrecht, London (2004), p.331.

23. A.I.Yanson, I.K.Yanson, J.M.van Ruitenbeek, *Nature (London, UK)*, **400**, 144 (1999).

24. V.Rajagopalan, S.Boussaad, N.J.Tao, *Nano Lett.*, **3**, 851 (2003).

25. C.Obermair, H.Kuhn, Th.Schimmel, *Beilstein J. Nanotechnol.*, **2**, 740 (2011).

26. J.O.M.Bockris, A.K.N.Reddy, Modern Electrochemistry, 2nd ed. Kluwer Academic Pub

27. A.Feher, A.A.Mamalui, A.Ya.Dul'fan et al., *Low Temp. Phys.*, **31**, 921 (2005).

28. Y.A.Kosevich, O.Y.Tkachenko, E.S.Syrkin, in: J.Archilla, F.Palmero, M.Lemos et al. (eds.), Nonlinear Systems, vol.2. Springer, Cham (2018).

29. M.L.Polyakov, A.Feher, E.S.Syrkin et al., *J. Mol. Liq.*, **127**, 65 (2006).

30. S.S.Braun, Elementary Processes in a Gas Discharge Plasma, Gostekhizdat, Moscow (1961) [in Russian].

31. P.N.Belkin, Electrochemical-thermal treatment of metals and alloys. Mir, Moscow (2005) [in Russian].

32. W.Benenson, J.W.Harris, H.Stocker, H.Lutz (eds.), Handbook of Physics. Springer, New York (2006).

33. P.G.Debenedetti, Metastable Liquids: Concepts and Principles, Princeton University Press, Princeton (1996).

34. I.M.Crichton, J.A.McGeough, *J. Appl. Electrochem.*, **15**, 113 (1985).

35. A.B.Khayry, J.A.McGeough, *Proc. R. Soc. London Ser. A*, **412**, 403 (1987).

36. E.P.Velikhov, V.S.Golubev, S.V.Pashkin, *Sov. Phys. Usp.*, **25**, 340 (1982).

37. J.Freidberg, Plasma Physics and Fusion Energy, Cambridge University Press, Cambridge, New York (2007).

38. P.H.Diamond, S.I.Itoh, K.Itoh, Modern Plasma Physics, vol. 1., Cambridge University Press, Cambridge, New York (2010).

39. A.A.Andronov, A.A.Vitt, S.E.Khaikin, Theory of Oscillators, Pergamon Press, Oxford, London, Edinburgh (1966).

40. A.Jenkins, *Phys. Rep.*, **525**, 167 (2013).

41. G.V.Kamarchuk, A.P.Pospelov, A.V.Savytskyi et al., *SN Appl. Sci.*, **1**, 244 (2019).